

Deformation-Induced Changes in the Structure of Fullerites C_{60/70} during Their Mechanical Activation

V. I. Lad'yanov, R. M. Nikonova, N. S. Larionova, V. V. Aksanova,
V. V. Mukhalin, and A. D. Rud'

Physical-Technical Institute, Ural Branch of the Russian Academy of Sciences,
ul. Kirova 132, Izhevsk, 426000 Republic of Udmurtia, Russia

e-mail: Nastasya2601@mail.ru

Received November 29, 2012

Abstract—Structural changes occurring during the mechanical activation of fullerites C_{60/70} have been investigated using X-ray diffraction, IR and UV spectroscopy, and scanning electron microscopy. The complete destruction modes of fullerite have been determined (3.5 h with the power density of the mill of 4.3 W/g and 28 h with 2.2 W/g). The destruction of the crystal structure of fullerites is accompanied by the destruction of fullerene molecules. The residual solvent, which enters into the composition of C_{60/70}, is retained during the entire time of mechanical activation. In this case, the low-frequency shift of absorption bands of toluene (729 → 725 cm⁻¹), which is caused by the deformation of the solvent molecule in the composition of crystal solvates, has been observed. It has been shown that the deformation stability of graphite is substantially lower than in the case of fullerite.

DOI: 10.1134/S1063783413060206

1. INTRODUCTION

Starting from the instant of discovery of fullerenes, they are widely used in biology and medicine, tribology, power engineering, metallurgy, etc. Great attention is paid to technologies of modifying metals to improve their properties and obtain new materials [1–3]. For this purpose, mechanical alloying (the mechanical synthesis MS) in ball mills is used [4–8]. The published data on the behavior of fullerites during the high-energy milling with the use of mills of various types are contradictory [4, 9–12]. Depending on the selection of mechanical activation (MA) conditions, particularly, the power density of the used mill and the medium of mechanochemical treatment (air, vacuum, and an inert medium), the formation of metastable crystalline/amorphous structures of carbon from “amorphous fullerite-like” carbon [4, 8–11] and “graphite-like” carbon [13] to “diamond-like” carbon [13] is possible. It is shown in [12, 13] that the temperature evolution of amorphous fullerites obtained during their MA can lead either to ordering the structure with the formation of the crystalline phase of fullerite or to the formation of the diamond-like amorphous phase (>600°C) depending on the power density and subsequent annealing.

It is known that structural variations of fullerites at high deformation loads can be accompanied by the formation of dimer structures. The formation of dimers C₁₂₀ is fixed during the MA of fullerites by a dry method [4, 10] as well as with the use of various catalysts [14–16]. In this case, an increase in density and a

decrease in the volume of the fcc lattice is observed because of connection of C₆₀ molecules with each other. There are the data on obtaining dimers C₁₄₀ difficult-to-obtain by other methods [17] and so-called crossed dimers C₁₃₀ [18].

During the MA of fullerites, their sorption properties vary, which makes it possible to obtain fullerene-containing compounds of various chemical compositions. For example, the MS of fullerites in the hydrogen medium is used when obtaining fullerene hydrides C₆₀H_n [11], in the oxidizing medium—for obtaining the mixtures of polyoxide fullerenes of various compositions C₆₀H_n [19, 20], etc. The MS of more complex modified fullerene structures with specified chemical properties is widely extended [21–25].

As the initial sample, both monofullerite C₆₀ (e.g., [9–12, 26]) and the more available mixture C_{60/70} [4, 9, 18] without additional separation of fullerite into fractions in the liquid chromatograph are used. Fullerite C_{60/70}, which is obtained by crystallization from the toluene solution, comprises molecular complexes C₆₀–C₇₀–C₆H₅CH₃ (crystal solvates), in which the molecules of fullerenes and the solvent are associated between each other by weak van der Waals forces. It is known that the removal of toluene is possible during prolonged annealings in conditions of dynamic vacuum (~200°C) and/or by the sample sublimation [27]. In this case, the behavior of toluene after the MA of fullerites C_{60/70} (the possibility of destruction of molecular complexes C₆₀–C₇₀–C₆H₅CH₃ during the

Composition of the initial mixture $C_{60}/70$ (wt %)

C_{60}	C_{70}	$C_{60}O, C_{60}O_2, C_{70}O$	$C_{76}, C_{78}, C_{82}, C_{84}$	Residual toluene
82.18	14.08	2.81	0.93	1.05

MA with the subsequent removal of residual toluene) was not considered in publications.

Comparative investigations of the deformation behavior of fullerite and other forms of carbon, for example, graphite and carbon nanotubes, performed in identical experimental conditions, are absent. The results of investigations of nanodimensional carbon, which is obtained during the MA of graphite, are particularly presented in [28–32], and the data for carbon nanotubes are presented, for example, in [33–35]. To synthesize nanostructured carbon, authors of [11] suggested using fullerite as the less stable carbon phase compared with graphite as the precursor.

In this study, we present the results of investigation into the structural variations in fullerenes $C_{60}/70$ as well as in graphite during their MA in an AGO-2S ball planetary mill.

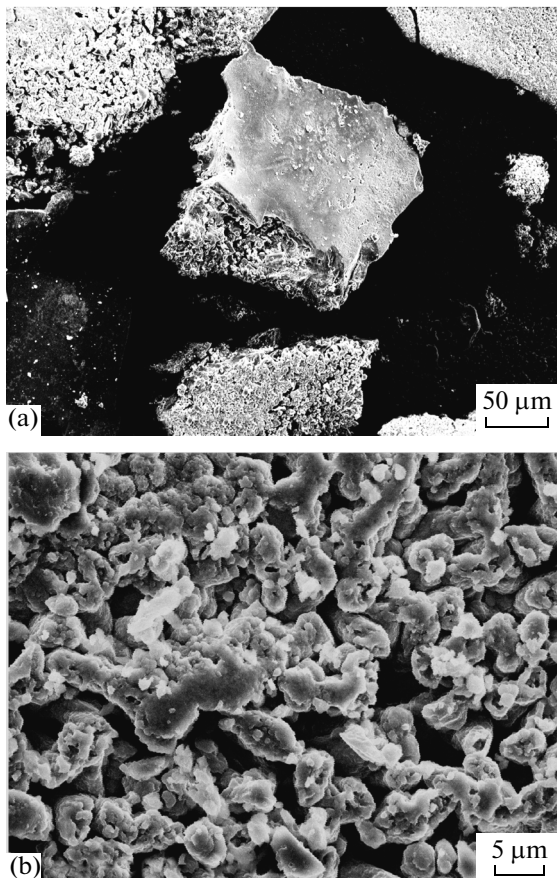


Fig. 1. General appearance of fullerenes $C_{60}/70$.

2. MATERIALS AND EXPERIMENTAL TECHNIQUE

Investigations were performed for fullerenes obtained at Physical–Technical Institute of the Ural Branch of the Russian Academy of Sciences by electric-arc evaporation of graphite rods with the subsequent extraction of fullerenes from the fullerene-containing ash by boiling toluene in a Soxhlet device and the further crystallization of fullerite from the solution in the rotation evaporator and for shaving-like graphite obtained by mechanical milling the rods of the osch. 7-2 grade. The composition of the initial mixture $C_{60}/70$ (by the data of highly efficient liquid chromatography and thermal gravimetry)¹ is presented in the table. The MA was performed in an AGO-2S ball planetary mill (the drums are made from hardened stainless steel #40Kh13#, and the balls 8 mm in diameter were made of steel #ShKh15#). The MA of fullerenes $C_{60}/70$ was performed at power densities of 2.2 and 4.3 W/g in an inert medium ($P_{Ar} = 0.1$ MPa) with preliminary evacuation ($P = 10^{-3}$ MPa). The MA duration was 0.4–28 h.

The X-ray structural studies of the samples before and after the MA were performed using a BRUKER D8 ADVANCE diffractometer ($CuK\alpha$ radiation). The stability of the molecular state of fullerenes was determined by the data of the IR and UV spectroscopy as well as by using the qualitative chemical analysis. In the last case, the samples under study were dissolved in toluene, and the presence or absence of fullerenes in the sample was judged by the intensity of solution coloration. The IR studies were performed using an FSM 1202 Fourier spectrometer with the resolution of 1 cm^{-1} (14 scans). To obtain the transmission spectra, the pelleted samples of fullerene powders with KBr in the ratio of 1 : 250 mg were prepared. The stability of molecules of the fullerene mixture after the MA was evaluated quantitatively using the absorption spectrophotometry (Lambda650, fullerene solutions in toluene) with molar absorption coefficients for 400, 410, and 472.8 nm calculated in [36]. The electron microscopy investigations were performed using a Jeol JSM 6360LA scanning electron microscope.

3. RESULTS AND DISCUSSION

The initial mixture of fullerenes $C_{60}/70$ consists of plane crystals 200–800 μm in size (Fig. 1a) with a developed loose surface (Fig. 1b). During initial milling times in a mill, the uniform stirring and agglomeration of the particles up to 200 μm in size occur (Fig. 2a). The further deformation effects lead to milling these agglomerates to 2 μm (after 24-h MA, Fig. 2d).

¹ A mixture of fullerenes $C_{60}/70$ is analyzed by E.V. Skokan at the Department of Chemistry of the Moscow State University.

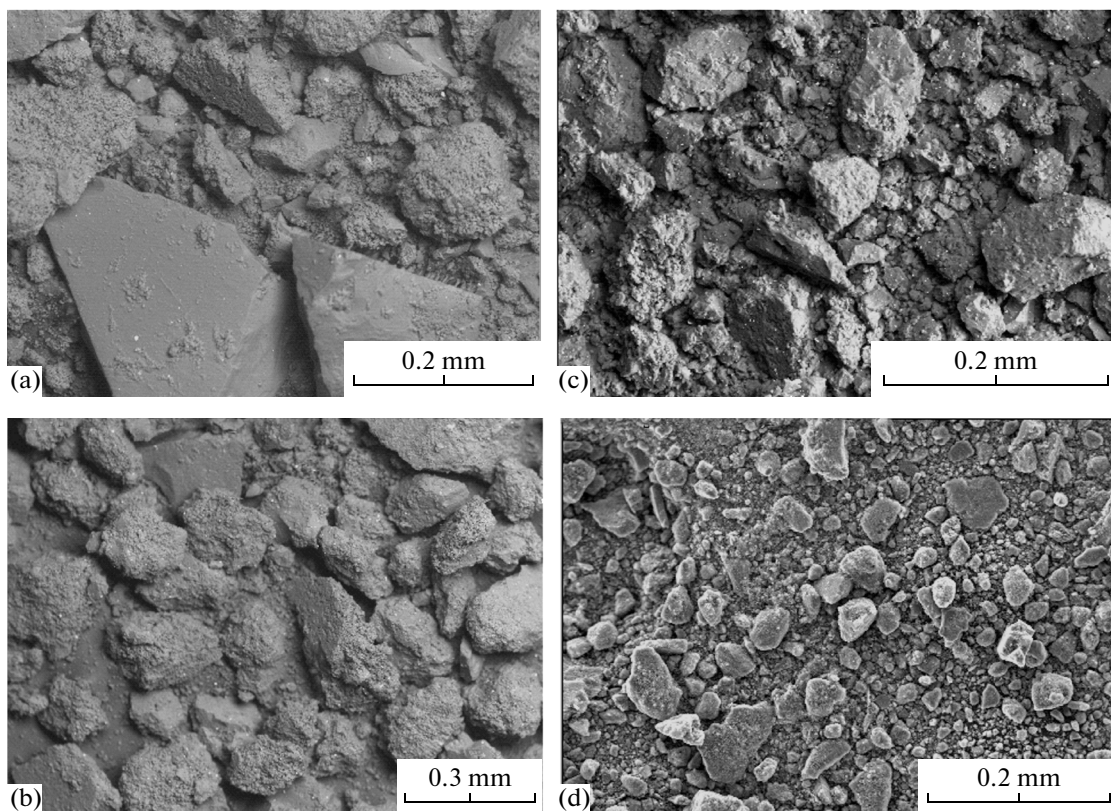


Fig. 2. Change of dispersity of powders $C_{60/70}$ after their MA for (a) 2, (b) 8, (c) 16, and (d) 24 h.

Figure 3 shows the X-ray diffraction patterns of mechanically activated fullerenes $C_{60/70}$ at two values of the power density of the mill (4.3 and 2.2 W/g). An increase in the MA time of the samples leads to a considerable decrease in intensity of diffraction lines and their broadening, which indicates the disordered crystal structure of fullerenes. During intense ball milling, mixture $C_{60/70}$ remains stable for 2 and 8 h at power densities of the mill of 4.3 and 2.2 W/g, respectively. The further milling the samples leads to the appearance of amorphous halos in the X-ray diffraction patterns, which are situated in the region of fundamental peaks of fullerenes ($2\theta \sim 8$ and 18°). As the MA time increases to 3.5 and 28 h for 4.3 and 2.2 W/g, respectively, the halo maximum shifts towards the fundamental peak of graphite (line (002), $\sim 25^\circ$), and corresponds to ash in this case, which indicates the complete destruction of the crystal structure of $C_{60/70}$. According to [11], the above-described states correspond to “amorphous fullerite-like” and “amorphous graphite-like” phases.

At milling times shorter than 3.5 h (4.3 W/g), the powders are soluble in toluene with its characteristic coloration (inset in Fig. 4); in this case, as the MA time increases, the coloration intensity of the solution decreases. This means that not only the crystal structure of fullerenes but also fullerene molecules are

destructured during milling in the ball planetary mill. A considerable decrease in intensity of fundamental absorption bands of C_{60} and C_{70} is observed in the IR spectra of samples $C_{60/70}$ (Fig. 4). After the 24-h MA (2.2 W/g), only strongest modes corresponding to C_{60} are retained in the spectrum, and after the 28-h MA, their absence is observed, which indicates the complete destruction of fullerenes. In this case, no noticeable oxidation of fullerenes as well as formation of dimers is observed.

The qualitative evaluation of the fullerene content in the samples after their MA, which was fulfilled by the UV spectral analysis, showed (Fig. 5) that fullerene molecules remain completely stable for the activation time up to 1 h at 4.3 W/g and 2–4 h at a lower value of the power density of the mill (2.2 W/g). The MA time of 3.5 and 28 h, respectively, is necessary for the complete destruction of the molecular structure. As it was shown above, after these milling times, the amorphous fullerite-like structure transforms into amorphous graphite-like structure.

It is known [27, 37] that fullerenes crystallized from the toluene solution absorb the residual solvent. The structural state of the samples of the mixtures obtained by recrystallization in the evaporator is characterized by the presence of two phases, namely, fcc- C_{60} and $C_{60}-C_{70}-C_6H_5CH_3$, in which molecules of fullerenes

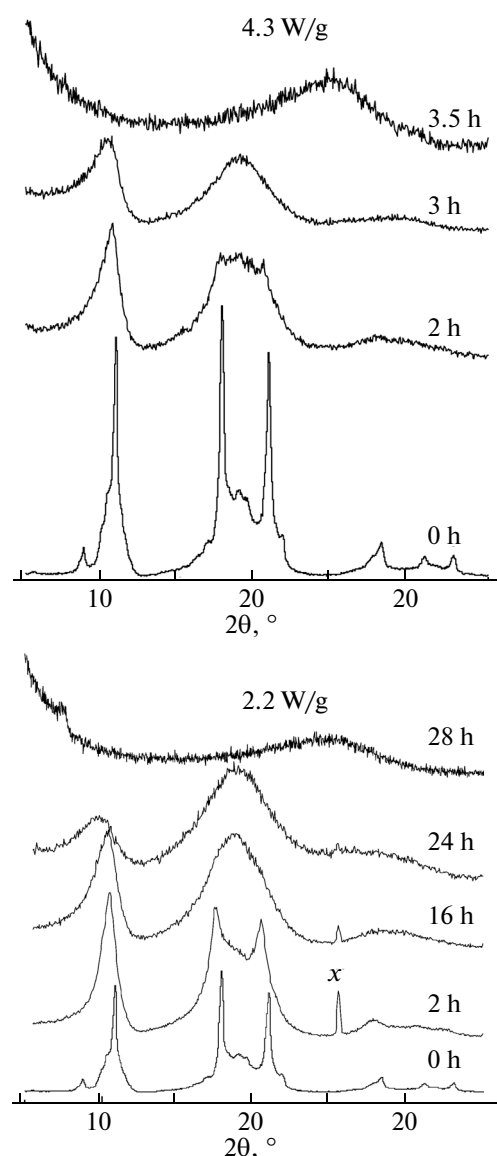


Fig. 3. Influence of the power density on destruction of fullerites $C_{60/70}$ (x is the cuvette material).

and the solvent are associated between each other by weak van der Waals forces. According to the IR spectroscopy data, the solvent is retained in the sample composition for the entire MA time after the MA of fullerites $C_{60/70}$, which is indicated by the presence of the absorption band at $\sim 725 \text{ cm}^{-1}$ (Fig. 4). During the MA, a planar toluene molecule is deformed [38], which manifests itself in the IR spectrum in the shift of absorption bands (ABs) of toluene. Figure 6 represents the fragments of MA spectra of the mixture $C_{60/70}$ normalized to the transmission intensity of the background. For comparison, the IR spectrum of the KBr pellet compacted with toluene without fullerite $C_{60/70}$ is presented. The location of the ABs corresponds to the deformation symmetric vibration C–H of the aro-

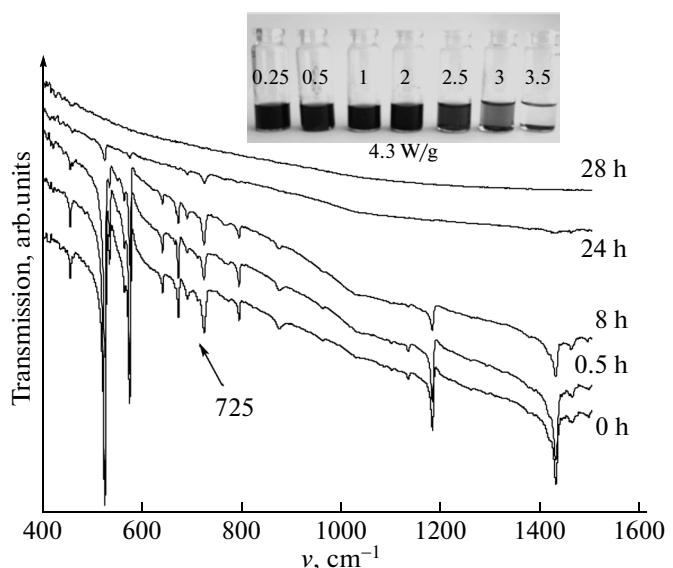


Fig. 4. IR spectra of fullerites $C_{60/70}$ after various MA times with the power density of 2.2 W/g. The qualitative chemical analysis of the solution of fullerites $C_{60/70}$ in toluene (4.3 W/g) is in inset, the digits correspond to MA times (in hours).

matic ring ($\delta_s(\text{C–H})$) of 729 cm^{-1} . In the presence of the molecular complex $C_{60}–C_{70}–C_6\text{H}_5\text{CH}_3$, the low-frequency shift $729 \rightarrow 725 \text{ cm}^{-1}$ (the initial sample, curve 1), which is caused by the deformation of the molecule, is observed. During the MA, the location of ABs varies (curve 2) due to the variations in the crystal solvate structure. With the milling duration of 24 h, the AB shift decreases to 726 cm^{-1} (curve 3), which allows us to assume weakening the van der Waals interactions between the molecules of the complex $C_{60}–C_{70}–C_6\text{H}_5\text{CH}_3$ and its destruction. After 28-h milling, the sample contains no residual toluene.

Comparative investigations of fullerites $C_{60/70}$ and graphite showed substantial distinctions in their deformation behavior. After opening the drums after the 4-h MA, graphite powders burned, while fullerite powders did not burn. In order to exclude ignition of the samples, graphite powders were passivated with heptane upon opening the drums. Ignition indicates to considerably larger specific surface area of graphite powders as well as on the presence of opened dangling bonds, which promote the oxidation reaction upon the access of air oxygen. It is seen from Fig. 7 that amorphization of graphite occurs considerably earlier than that of fullerite. Already after the 1-h MA, an amorphous halo is observed in the X-ray diffraction pattern, while fullerite retains high crystallinity. In order to attain the same structural state as in the case of graphite, deformation effects on fullerite 28 h long are required (Fig. 7). Thus, despite the fact that graphite is the most thermodynamically stable carbon phase, its

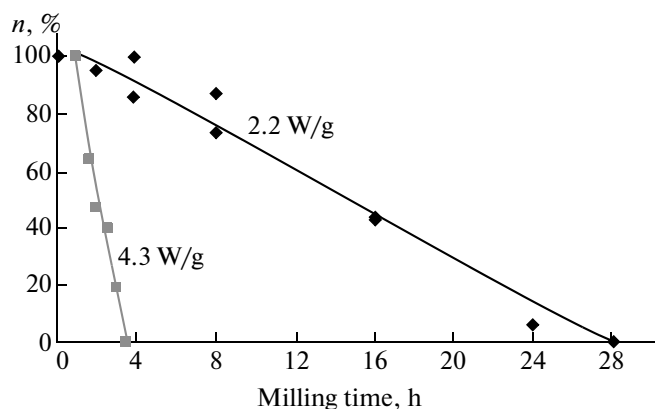


Fig. 5. Variation in the weight fraction n of fullerenes with time in different MA modes.

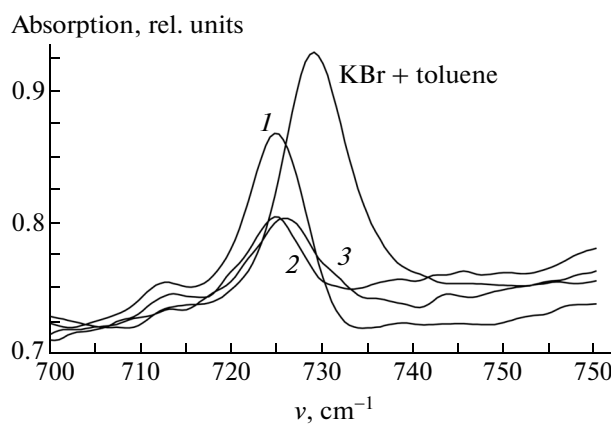


Fig. 6. Fragments of IR spectra of mechanically activated powders of mixture $C_{60}/70$. (1) Starting powder, (2) after the 16-h MA, and (3) after the 24-h MA.

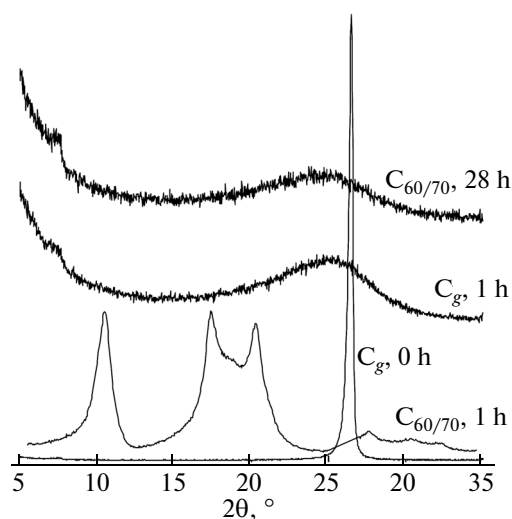


Fig. 7. X-ray diffraction patterns of the comparison of the samples after the MA of graphite C_g (0 and 1-h MA) and fullerite $C_{60}/70$ (1 and 28-h MA).

deformation stability is substantially lower than that of fullerite.

The observed distinctions in the deformational instability of graphite and fullerite are apparently associated with the different bond strength between carbon atoms. The length of the C–C bond inside the plane of graphite layers is 0.1415 nm, and neighboring layers of carbon atoms in the crystal are at a rather long distance from one another (0.335 nm). This indicates the low bond strength between carbon atoms arranged in different layers. Differences in bond lengths inside the graphite plane and between the planes determine strong anisotropy of graphite properties. The low mechanical strength of graphite and its rapid amorphization are explained by this fact. In the case of fullerite, bond lengths inside the fullerene molecules are considerably shorter, namely, double ($C=C$) and single ($C–C$) bonds have the length 0.139 ± 0.001 and 0.144 ± 0.001 nm, respectively. Strong covalent bonds $C–C$ and $C=C$ promote retaining the molecules C_{60} and C_{70} themselves. According to the data of the quantitative UV analysis, the weight fraction of fullerenes after the 1-h MA is conserved equal to 100%, and after the 16-h MA, it decreases to 50% (Fig. 5). With the conservation of the structure of fullerenes, their crystallinity is also conserved.

4. CONCLUSIONS

Thus, performed investigations with the use of X-ray diffractometry, IR and UV spectroscopy, and scanning electron microscopy allowed us to conclude the following.

(i) Intense deformation effects, which are implemented during the MA of fullerites $C_{60}/70$, lead to their amorphization. In this case, the deformation stability is determined by the selected mode of the power density of the mill. It is established that the complete destruction of fullerite corresponds to the 3.5-h MA with the power density of the mill of 4.3 W/g and the 28-h MA at 2.2 W/g.

(ii) Deformation-induced destruction of the crystal structure of fullerites is accompanied by the destruction of fullerene molecules.

(iii) The residual solvent, which enters the composition of $C_{60}/70$, is retained during the entire MA treatment. The low-frequency shift of the toluene AB ($729 \rightarrow 725 \text{ cm}^{-1}$), which is caused by the deformation of the solvent molecule in the composition of crystal solvates, is observed in this case.

(iv) It is shown that the deformation stability of graphite is substantially lower than that of fullerite, which is apparently associated with the difference in the bond strength between carbon atoms.

ACKNOWLEDGMENTS

This study was supported by the Presidium Program of the Ural Branch of the Russian Academy of Sciences (project no. 12-T-2-1015).

REFERENCES

1. A. V. Eletskii, Phys.—Usp. **50** (3), 225 (2007).
2. V. N. Ivanova, J. Struct. Chem. **41** (1), 135 (2000).
3. C. Suryanarayana, Prog. Mater. Sci. **46**, 1 (2001).
4. M. Umemoto, Z. G. Liu, K. Masuyama, and K. Tsuchiya, Mater. Sci. Forum **312–314**, 93 (1999).
5. F. C. Robles Hernández, J. Metall. **10** (2), 107 (2004).
6. B. Lohse, A. Calka, and D. Wexler, J. Mater. Sci. **42** (2), 669 (2007).
7. X. Liu, Y. Liu, X. Ran, J. An, and Z. Cao, Mater. Charact. **58**, 504 (2007).
8. R. M. Nikonova, N. S. Pozdeeva, V. I. Lad'yanov, Khim. Fiz. Mezoskopiya **13** (1), 88 (2011).
9. Z. G. Liu, H. Ohi, K. Masuyama, K. Tsuchiya, and M. Umemoto, J. Phys. Chem. Solids **61**, 1119 (2000).
10. T. Braun, H. Rausch, L. P. Biro, E. Zsodos, R. Ohmacht, and L. Mark, Chem. Phys. Lett. **375**, 522 (2003).
11. A. V. Talyzin and A. Jacob, J. Alloys Compd. **395**, 154 (2005).
12. V. P. Glazkov, S. S. Agafonov, I. F. Kokin, and V. A. Somenkov, in *Abstracts of Papers of the XI International Conference "Hydrogen Materials Science and Chemistry of Carbon Nanomaterials" (ICHMS'2009)*, Yalta, Crimea, Ukraine, August 25–31, 2009, p. 753.
13. S. S. Agafonov, V. P. Glazkov, I. F. Kokin, and V. A. Somenkov, Phys. Solid State **52** (6), 1329 (2010).
14. G.-W. Wang, K. Koichi, Y. Murata, and M. Shiro, Nature (London) **387** (5), 583 (1997).
15. K. Komatsu, G.-W. Wang, Y. Murata, T. Tanaka, and K. Fujiwara, J. Org. Chem. **63**, 9358 (1998).
16. K. Komatsu, K. Fujiwara, T. Tanaka, and Y. Murata, Carbon **38**, 1529 (2000).
17. D. V. Konarev, S. S. Khasanov, I. I. Vorontsov, G. Saito, and A. Otsuka, Synth. Met. **135–136**, 781 (2003).
18. K. Komatsu, K. Fujiwara, and Y. Murata, Chem. Commun. (Cambridge) **17**, 1583 (2000).
19. H. Watanabe, E. Matsui, Y. Ishiyama, and M. Senna, Tetrahedron Lett. **48**, 8132 (2007).
20. J. Zhang, K. Porfyrakis, M. R. Sambrook, A. Ardavan, and G. A. D. Briggs, J. Phys. Chem. B **110** (34), 16979 (2006).
21. G.-W. Wang, in *Encyclopedia of Nanoscience and Nanotechnology*, Ed. by H. S. Nalwa (American Scientific, Valencia, California, United States, 2004), Vol. 3, p. 557.
22. K. Fujiwara and K. Komatsu, Org. Lett. **4** (6), 1039 (2002).
23. Y. Murata, A. Han, and K. Komatsu, Tetrahedron Lett. **44**, 8199 (2003).
24. Y. Murata, N. Kato, and K. Komatsu, J. Org. Chem. **66**, 22, 7235 (2001).
25. F. Constabel and K. E. Geckeler, Tetrahedron Lett. **45**, 2071 (2004).
26. E. V. Skokan, V. E. Alioshina, F. M. Spiridonov, I. V. Arkhangelsky, V. Ya. Davydov, N. B. Tamm, and L. N. Sidorov, J. Phys. Chem. **99**, 16116 (1995).
27. E. A. Eremina, V. I. Lad'yanov, and R. N. Nikonova, Russ. J. Phys. Chem. A **82** (13), 2207 (2008).
28. X. H. Chen, H. S. Yang, G. T. Wu, M. Wang, F. M. Deng, X. B. Zhang, J. C. Peng, and W. Z. Li, J. Cryst. Growth **218**, 57 (2000).
29. N. J. Welham, V. Berbenni, and P. G. Chapman, Carbon **40** (13), 2307 (2002).
30. R. Janot and D. Guerard, Carbon **40**, 2887 (2002).
31. N. J. Welham, V. Berbenni, and P. G. Chapman, J. Alloys Compd. **349**, 255 (2003).
32. J. L. Li, L. J. Wang, and W. Jiang, Appl. Phys. A: Mater. Sci. Process. **83**, 385 (2006).
33. Y. B. Li, B. Q. Wei, J. Liang, Q. Yu, and D. H. Wu, Carbon **37**, 493 (1999).
34. H. Pan, L. Liu, Z. X. Guo, L. Dai, F. Zhang, D. Zhu, R. Czerw, and D. L. Carroll, Nano Lett. **3** (1), 29 (2003).
35. L. Chen, H. Xie, Y. Li, and W. Yu, J. Nanomater. **2008**, 783981 (2008).
36. M. I. Maistrenko, N. S. Anikina, A. D. Zolotarenko, E. A. Lysenko, G. A. Sivak, and D. V. Shchur, in *Abstracts of Papers of the VIII International Conference "Hydrogen Materials Science and Chemistry of Carbon Nanomaterials" (ICHMS'2003)*, Sudak, Crimea, Ukraine, September 14–20, 2003, p. 596.
37. M. A. Eremina, R. M. Nikonova, V. I. Lad'yanov, and V. V. Aksanova, Russ. J. Phys. Chem. A **83** (11), 1924 (2009).
38. K. T. Antonova, M. K. Marchewka, E. Kowalska, and P. Byszewski, Vib. Spectrosc. **16**, 31 (1998).

Translated by N. Korovin

SPELL: OK